Journal of Alloys and Compounds 480 (2009) 70–72

Contents lists available at ScienceDirect

Journal of Alloys and Compounds

journal homepage: www.elsevier.com/locate/jallcom

Synthesis and characterization of needle-like $IrSe_2$ microrods

C.H. Liang[a], Y.H. Chan[a], K.K. Tiong[b,*], Y.S. Huang[b], D.O. Dumcenco[b], P.C. Liao[c]

[a] Department of Electrical Engineering, National Taiwan Ocean University, Keelung 202, Taiwan
[b] Department of Electronic Engineering, National Taiwan University of Science and Technology, Taipei 106, Taiwan
[c] Department of Electronic Engineering, Technology and Science Institute of Northern Taiwan, Taipei 106, Taiwan

ARTICLE INFO

Article history:
Received 26 June 2008
Received in revised form
12 September 2008
Accepted 15 September 2008
Available online 25 November 2008

PACS:
71.20.Be
81.10.−h
72.15.Eb
68.37.Hk

Keywords:
Transition metal alloys and compounds
Crystal growth
Electrical transport
SEM

ABSTRACT

Needle-shape $IrSe_2$ microrods, with maximum thickness of 6 μm, maximum width of 17 μm, and 20 mm in length were synthesized by the chemical vapour transport method with ICl_3 as the transporting agent. Energy-dispersive X-ray spectroscopy showed an atomic Ir to Se ratio of $1:(2-\delta)$, where $0 < \delta < 0.09$. Scanning electron microscopy showed single crystalline structure for the synthesized $IrSe_2$. The electrical properties of the $IrSe_2$ were studied via temperature dependent transport properties measurements in the range of 20–510 K. The thermal band gap was evaluated to be 0.17 eV. Room temperature Hall effect measurement showed p-type semiconducting character for the sample.

© 2008 Elsevier B.V. All rights reserved.

1. Introduction

Iridium diselenide crystallizes with a tridimensional marcasite-type structure and belong to the p_{nma} $\left(D_{2h}^{16}\right)$ space group [1,2]. The average Ir–Se bond distance is equal to 2.476 Å and the long bond length in the chalcogen pairs is $d_{se-se} = 2.555$ Å [2,3]. To date, only few works on the electrical [4] and vibrational properties [3] of the materials have been reported. Morsli et al. [4] had reported for the first time the temperature dependence of the conductivity for polycrystalline $IrSe_2$. However, they failed in their attempt to measure the room temperature Hall effect. The failure has been attributed to the extremely low Hall coefficient due to opposite contribution of holes and electrons at room temperature.

In this article, we report the preparation and characterization of $IrSe_2$ single crystals, as indicated by the scanning electron microscopy (SEM), with naturally formed needle-like microrods. Energy dispersive X-ray spectroscopy (EDX) was performed to determine the stoichiometry of the sample. The marcasite-type structure for the synthesized crystal structure was confirmed by the X-ray diffraction (XRD) patterns. We have also reported an elaborate study of the temperature dependence of the transport properties of $IrSe_2$ over an extended range from 20 to 510 K. The mechanisms affecting the temperature dependence of the transport properties were discussed and analyzed.

2. Experimental

The synthesis of $IrSe_2$ microrods (μRs) was undertaken using the method of chemical vapour transport with ICl_3 as the transporting agent. The transport agent and the elements (Ir: 99.99% pure, Se: 99.999%) were evacuated and sealed inside a clean quartz tube. To improve the stoichiometry, selenium with 2 mol% in excess was added with respect to iridium. The quartz tube was placed in a three-zone furnace and the charge prereacted at 700 °C for 72 h with the growth zone at 900 °C for 240 h, preventing the transport of the product. The furnace was then equilibrated to give a constant temperature across the reaction tube, and was programmed over 24 h to give an optimal temperature gradient of about 1080 → 1030 °C at which single crystal growth took place. SEM investigations were done employing a field-emission scanning electron microscope model JEOL-JSM6500F using an acceleration voltage = 15 kV, while EDX was performed using the same set up fitted with an OXFORD INCA Energy 300 spectrometer. The crystal structure is analyzed by the Rigaku RTP300RC powder X-ray diffractometer using Ni-filtered CuKα radiation with λ = 1.5418 Å experimentally calibrated by a silicon standard. The XRD patterns were recorded by means of a slow-moving radiation detector. The lattice parameters were determined by the least-squares fit of SigmaPlot mathematical software [5]. The best fitting result leads to a standard deviation within ±0.01% and confirmed the orthorhombic symmetry of $IrSe_2$ [1,2]. For the conductivity measure-

* Corresponding author. Tel.: +886 2 24622192x6208; fax: +886 2 24635408.
E-mail address: b0114@mail.ntou.edu.tw (K.K. Tiong).

0925-8388/$ – see front matter © 2008 Elsevier B.V. All rights reserved.
doi:10.1016/j.jallcom.2008.09.179

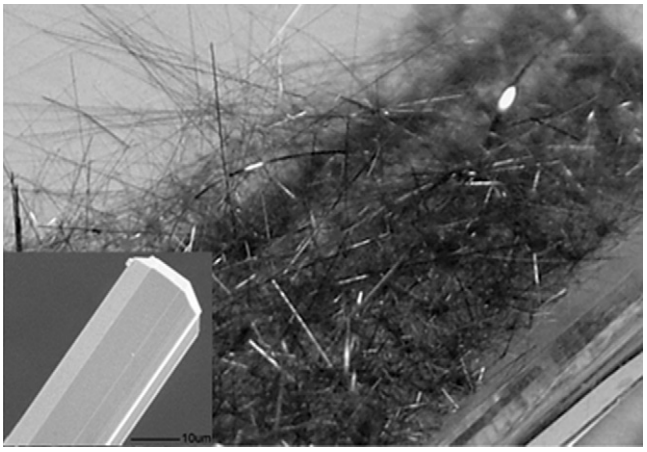

Fig. 1. Morphology of the as-grown sample. Inset is a high magnification SEM image of a selected microrod.

ments, the single crystals were rinsed successively with Aqua regia and deionizer water and electrical connections to the crystal were made by means of gold wires and attached to the crystal surface by means of conducting silver paint. The ohmic nature of the contacts was confirmed by the current–voltage (I–V) characteristics, which appeared linear and independent of the reversal current for low applied voltages.

3. Results and discussion

Fig. 1 shows morphology of the sample, from which a large number of needle-like microrods can be observed. The high magnification SEM image of a selected microrod (in the inset in Fig. 1) showed the synthesis of single crystalline orthorhombic $IrSe_2$ sample. The thickness of the $IrSe_2$ μRs varies from 3 to 6 μm, with maximum width of 17 μm, and lengths up to 20 mm. The chemical composition of the sample was analyzed by EDX, showing an atomic Ir to Se ratio of $1:(2-\delta)$, with $0<\delta<0.09$ denoting the slight selenium deficiency of the sample. The small deviation of the atomic ratio can vary from point to point as well as from sample to sample. This weak non-stoichiometry as mentioned by Morsli et al. [4] has to be considered to explain the conductivity by hopping.

From the XRD patterns (figure not shown), the values of lattice parameters of the as-grown samples are fitted to be $a = 21.16 \pm 0.05$ Å, $b = 5.88 \pm 0.01$ Å, and $c = 3.73 \pm 0.01$ Å. These numbers differ slightly from the previously reported values of $a = 20.94$ Å, $b = 5.93$ Å, and $c = 3.74$ Å [1,2].

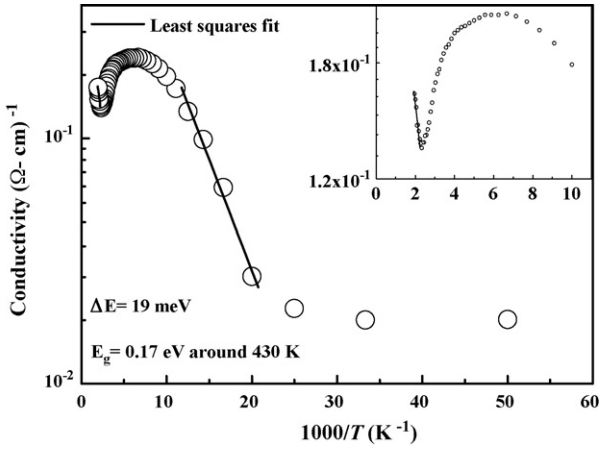

Fig. 2. The temperature dependent electrical conductivity of $IrSe_2$. Inset is the expanded view of the conductivity at high temperature.

Displayed in Fig. 2 (hollow circles) is the electrical conductivity (σ) of $IrSe_2$ as a function of temperature in the range between 20 and 510 K. From Fig. 2, the conductivity of the samples increases with the increase of the temperature. The increase of conductivity in the temperature range 50–90 K is attributed to the ionization effect of impurities and can be expressed as [6]:

$$\sigma = \sigma_0 \exp\left(\frac{-\Delta E}{kT}\right) \quad (1)$$

where ΔE is the carriers activation energy. The $\ln\sigma$ vs. $1000/T$ graphs show the linear region where the slope yields carriers activation energy to be $\Delta E = 19 \pm 0.5$ meV for $IrSe_2$. At temperature higher than 90 K, the temperature dependence of conductivity deviates from linearity and attains a local maximum (full ionization of impurity carriers) of $\sigma = 0.214\ \Omega^{-1}\,cm^{-1}$ at 150 K. The nonlinearity of conductivity may be attributed to the contribution from the thermally activated hopping of small polarons associated with the non-stoichiometry of the narrow band gap material [2,4]. Beyond 150 K, the conductivity subsequently decreases (due to electron–phonon scattering effect) for temperature increases up to $T_i = 430$ K. The temperature T_i corresponds to the onset of ionization temperature for intrinsic carriers over the thermal band gap of $IrSe_2$. A second linear region exists in the 430–510 K temperature range (inset in Fig. 2) where conductivity increases rapidly to $0.161\ \Omega^{-1}\,cm^{-1}$ at 510 K. The temperature dependent conductivity in the intrinsic region as a result of thermal activation of carriers across the energy gap E_g [6,7] can be written as

$$\sigma = \sigma_0 \exp\left(\frac{-E_g}{2kT}\right) \quad (2)$$

where σ_0 is a constant. From the $\ln\sigma$ vs. $1000/T$ plots the slope of the second linear region give the value of thermal band gap to be 0.17 ± 0.02 eV. The obtained value is about half that of the assumed temperature independent $E_g = 0.33$ eV by Morsli et al. [4].

For the as-grown sample, we were also able to perform the Hall effect measurements, which indicate p-type semiconducting behaviour of $IrSe_2$ single crystals with room temperature Hall mobility and carrier concentration of $31\ cm^2\,V^{-1}\,s^{-1}$ and $7.9 \times 10^{16}\ cm^{-3}$, respectively. These results differed considerably with that of Morsli et al. [4], where compensated n-type $IrSe_2$ was reported and they failed in their attempt to measure the room temperature Hall mobility. The different electrical transport properties are most likely due to the different growth technique and the type of transport agent used in the growth process.

4. Summary

In summary, we have demonstrated the synthesis of single crystals $IrSe_2$ μRs with thickness of about a few micrometer, maximum width of 17 μm and 20 mm in length by chemical vapour transport method using ICl_3 as a transporting agent. SEM image shows the synthesis of microrods with orthorhombic symmetry and the EDX analysis indicates nonuniform weak non-stoichiometry of the as-grown samples. The electrical transport properties of $IrSe_2$ were studied via the temperature dependent conductivity measurements. The carrier activation energy was evaluated to be 19 meV. The high temperature conductivity measurement yielded a thermal band gap of 0.17 eV and the room temperature Hall measurements showed p-type semiconducting behaviour with mobility equal to $31\ cm^2\,V^{-1}\,s^{-1}$.

Acknowledgements

The authors acknowledge the support of the National Science Council of Taiwan under the projects nos. NSC 96-2112-M-019-003 and NSC 96-2112-M-011-001.

References

[1] L.B. Barricelli, Acta. Crystallogr. 11 (1958) 75–79.
[2] S. Jobic, P. Deniard, R. Brec, J. Rouxel, M.G.B. Drew, W.I.F. David, J. Solid State Chem. 89 (1990) 315–327.
[3] C. Sourisseau, R. Cavagnat, M. Fouassier, S. Jobic, P. Deniard, R. Brec, J. Rouxel, J. Solid State Chem. 91 (1991) 153–172.
[4] M. Morsli, A. Bonnet, Y. Tregouet, A. Conan, S. Jobic, R. Brec, Appl. Surf. Sci. 50 (1991) 500–504.
[5] SigmaPlot for windows Version 9.0 (Systat Software, Inc.), 2004.
[6] K.K. Tiong, C.H. Ho, Y.S. Huang, Solid State Commun. 111 (1999) 635–640.
[7] S.M. Sze, Semiconductor Devices: Physics and Technology, Bell Tel. Lab. Inc., New Jersey, 1985, p. 16.